A Model Predictive Control for Microgrids Considering Battery Aging

Ugur Can Yilmaz, Mustafa Erdem Sezgin, and Murat Gol

Abstract—The increasing number of distributed energy resources (DERs), advancing communication and computation technologies, and reliability concerns of the customers have caused an intense interest in the concept of microgrid. Although DERs are the biggest motivation of the microgrids due to their intermittent generation characteristics, they constitute a risk for system reliability. Battery storage systems (BSSs) stand as one of the most effective solutions for this reliability problem. However, the inappropriate use of BSS creates other operational problems in power systems. In order to deal with these concerns explicitly in microgrids, an optimized microgrid central controller (MGCC) is the key factor, which controls the real-time operation of a microgrid. This work proposes a model predictive control (MPC) based MGCC that will provide optimal control of the microgrid, considering economic and operational constraints. The proposed system will minimize the energy cost of the microgrid by utilizing mixed-integer linear programming (MILP) assuming the presence of DERs and BSS as well as the bi-directional grid connection. Moreover, the aging effect of BSS will be considered in the proposed optimization problem which will provide an up-to-date system model. The proposed method is evaluated using real load and photovoltaic (PV) generation data.

Index Terms—Microgrid, optimization, battery storage, model predictive control, mixed-integer linear programming.

I. INTRODUCTION

WITH the developments in photovoltaic (PV) panel and wind turbine technologies, energy generation becomes easier and more environmental friendly compared to the conventional methods. Those sources are connected to the grid with small amounts at various locations, and are called distributed energy resources (DERs). DERs make it possible to supply the load even if there is an interruption at the power grid, and to reduce the net power drawn from the grid during normal operation. However, it has been seen that some problems may arise due to the uncertainty in generation characteristics of DERs [1]. Although it is technically possible to eliminate these problems by virtue of the improvements in the storage technologies, it is not a simple task to solve all those issues.

The developments in DER technologies and introduction of new system elements such as energy storage systems make it possible to build an isolated system structure. These self-contained structures are known as microgrids. These systems have their own controller, and depending on the power quality at the point of common coupling, they may operate in the island mode for a certain time. Although microgrids offer high operational flexibility, their control is harder than the conventional grids, due to their low inertia and fast dynamic characteristics.

In microgrids, the intermittent characteristic of DERs creates some concerns about the reliability. To overcome these problems, the real-time control strategy of the microgrid, which is the microgrid central controller (MGCC), should be studied carefully. During the normal operation state of the grid, MGCC functions to minimize the operation cost of the microgrid. This work develops a control strategy for the normal operation state of the microgrid (on-grid operation), which constitutes the majority of the operation.

There are various works in the literature about the microgrid control in normal operation state for cost optimization. According to [2], the secondary control can be divided into centralized and decentralized controls. References [3] and [4] can be given as the examples of decentralized control strategy. In these works, multi-agent systems are proposed to minimize the operation costs of the system by considering each generation unit individually. However, with this method, the optimum operation of the microgrid might be missed due to the self-autonomy of the agents, where they do not have a full knowledge of the whole system. Moreover, with this method, only the current state of the system is considered, i.e., no future predictions are included. Thus, the optimum operation in a daily base may be missed. In addition, there is a huge communication burden of the given approach in [4]. Although in [5], the given neural-network strategy is applicable for the grid-connected mode of operation of the microgrid, the optimum operation of the system cannot be guaranteed with this method. Note that [5] neglects the battery storage systems (BSS). In [6], the energy storage system is included in the microgrid system. However, the effect of the aging of BSS is not given.

Model predictive control (MPC) in microgrid applications has been studied by the researchers. In [7], a primitive example of MPC is given. Reference [8] is one of the successful

examples of the MPC applications in microgrid control, where the contribution of storage system is also included. Although a detailed study on mixed-integer linear programming (MILP) is given in this work, the aging of BSS is not considered. Moreover, the given PV generation forecasting strategy, which is support vector machine, can be improved with neural networks. Another application of MPC strategy is given in [9], where different types of DERs and BSSs are taken into account. Moreover, different system market options are included in the system. However, it is not clear how the battery model is obtained and the cost function of BSS is derived. Reference [10] uses a stochastic MPC method to control the microgrid with BSS. However, BSS is not monitored in real time and the battery aging is not considered at all. Reference [11] adds the BSS cost to the objective function. However, an empirical method is used in the solution procedure. In addition to those studies, [12] can be given as another implemented MPC example, without considering the aging of the batteries, neither. References [13] and [14] are two recent studies on microgrid control concept where distributed MPC is considered. Those studies do not update the battery model with time, and do not involve the aging of battery in the control problem. Reference [15] proposes an energy management system by introducing penalty factor for fast charging/discharging to limit battery aging. However, it does not utilize real-time measurements to update the battery model. Finally, in [16], expected lifetime of a battery is calculated for microgrid control using normal distribution curve rather than real-time measurements.

In general, battery aging is neglected in microgrid control problems, assuming that aggressive usage of the battery is prevented. However, in applications where deep discharge (harsh usage) is possible, the proposed method stands forward.

Battery employment is essential in microgrid applications because of the unreliable nature of the renewable sources. However, due to the high investment cost of BSS, those systems should be modeled precisely and considered in the cost optimization. Harsh usage of the battery might seem to minimize the operation cost for the short term; however, this type of operation will cause the replacement of the battery sooner than expected. Therefore, considering the battery aging in the optimization model is essential to optimize the total cost. In order to include BSS in the microgrid control problem, a wide variety of models has been developed with varying degrees of complexity such as electro-chemical models [17], [18], mathematical models [19], [20] and electrical models [21] - [24]. Among those studies, electrical circuit models are commonly used to estimate the behaviour of the battery [25].

This paper proposes an MPC based MGCC that considers the aging of BSS to minimize the operation cost of a microgrid with a PV system. The proposed method estimates the up-to-date BSS capacity using real-time measurements. To the best of the authors' knowledge, this is the first study that estimates the capacity of a BSS based on a numerical method using real-time data, rather than employing heuristic

models. The main contributions of this paper are as follows:

1) The methods in the literature identify battery parameters numerically once. Those methods neither update the parameters during the battery lifetime, nor the update is realized in a heuristic manner. The proposed method, on the other hand, updates the parameters periodically, using real-time measurements in a numeric manner.

2) Since the method uses real-time measurements, it is capable of identifying unexpected parameter changes due to exposure to excessive temperature, physical shock, etc. However, conventional heuristic methods cannot detect those unexpected changes, as they follow the expected behavior of the battery aging.

In this paper, to give a thorough approach to all parts, the work is divided into four parts. In Section I, the problem and its background are defined. All the introductory definitions are given in this part. In Section II, the proposed solution for the given problem is explained. The required derivations and formulations are given in this section. In Section III, the results of the proposed solution method are illustrated. The comparison of different operational cases are also given in this part. Finally in Section IV, the work is summarized and concluded.

II. PROPOSED METHOD

An MGCC to minimize the operation cost of the microgrid will be modeled for the operation of the system in normal operation state. To achieve this, the MPC method will be utilized, which enables an optimum solution for long-term operation. For simplicity, the losses in the microgrid and the losses in power electronic components are neglected. A detailed strategy about the inclusion of inverter and DC-DC converter losses can be found in [26]. In the considered system structure, it is assumed that the electric grid permits the bi-directional power flow, i.e., the excess power can be sold to grid with a different tariff. Furthermore, the effect of the aging of BSS, which directly affects the usable capacity of BSS, will be considered in this work. The optimization problem is formulated as an MILP problem.

The definition of MPC can be given as deciding the optimum control strategy for the current time instant based on forcasted behaviour of the system using dynamic models [27]. With this method, the control decision may not be the optimum operation for the current time instant. However, in the forecasted time horizon, the control decision yields the optimum solution based on the forecasted behaviour of the system.

In the system modeling, the PV generation model plays a crucial role. Generally, solar generation depends on the natural and environmental conditions such as temperature, fogginess, cloudiness, etc. Since the majority of commercial PV inverters have maximum power point tracking algorithm, it can be assumed that all the generated power is transferred to the microgrid. Although the PV generation can be used for the purpose of voltage regulation, this kind of usage will not be included in this work.

Load model is another key factor in modeling. Since it depends on the instantaneous choices of the people, it might be chaotic in small systems. One of the main purposes of microgrid operation is to provide uninterrupted service to the customers; therefore, it is not preferred to apply load shedding. Only in island mode of operation, some loads may be de-energized, but such a scenario will not be considered in this work.

Battery is the core of BSS and its optimal usage has an important role in cost optimization. Harsh usage of the BSS decreases the lifetime of the battery significantly. Therefore, in microgrid operation, the aging of the battery should be considered as well.

In this work, PV generation is forecasted using long-short term memory (LSTM), and load forecasting is performed using Kalman filter. Note that these forecasted results are used as inputs of the proposed MPC method, where the main contribution of this work is the integration of the BSS aging effect to MGCC, so that the proposed method will reduce the charging-discharging cycle numbers to expend the lifetime of BSS. In this work, a cycle is defined as discharging/charging period of the battery. In the discharging period, the state of charge (SoC) goes from 100% to 0%; while in the charging period, the SoC goes from 0% to 100%. In practical applications, the minimum SoC value may be limited to extend the lifetime of the battery. However, in order to emphasize the benefits of the proposed method, the given cycle definition is used. Note that 0% SoC does not indicate 0 open-circuit terminal voltage. The effect of aging on BSS capacity is estimated using least squares estimator, and expected lifetime of BSS is modeled as a function of the capacity. In this section, the load and generation forecasting methods are firstly presented. Then the proposed BSS capacity estimation method will be introduced, and it will be followed by the explanation of the proposed MGCC.

A. Load and PV Generation Forecasting

With the measured historical data, the load and PV generation characteristics of the microgrid can be forecasted easily. There are lots of different forecasting strategies in the literature for both problems. In [28] and [29], the use of artificial neural network (ANN) for load forecasting is proposed. In [29], the proposed ANN-based method can work with an accuracy of 99.5%. Also, auto-regressive integrated moving average (ARIMA) models have some popularity in literature, where they may be combined with some other methods [30], [31]. For the PV generation forecasting, there exist some methods based on Markov chain [32] as well as support vector machine [33], [34].

Although it is possible to use any method depending on the application, in this work, a Kalman filter based approach for load forecasting and LSTM method for PV generation forecasting will simply be utilized. The main motivations behind these choices are the ease of implementation and low memory requirements.

The results of the applied Kalman filter can be seen in Fig. 1, where the blue line represents the forecasted load,

and the red line represents the actual load measurement. Note that as the forecasting horizon changes, the time intervals employed for the Kalman filter change as well. Therefore, the forecasting may carry some inaccuracy, especially if there is an unexpected change in demand amount.
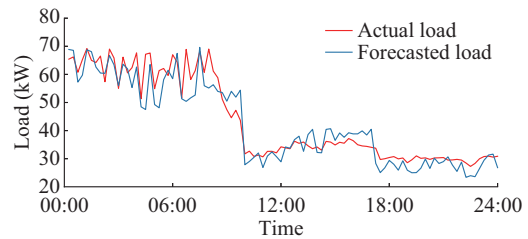

Fig. 1.   Comparison of actual and forecasted loads.

To forecast the PV generation, LSTM method is applied by using the LSTM tool of MATLAB. The employed forecasting tool receives the recorded PV generation values corresponding to the previous time instant and corresponding to the same time instant to be forecasted of the previous day. However, if cloudiness data is available, it can be used to improve the output of the LSTM method. The result can be seen in Fig. 2, where the red line represents the actual PV generation, and the blue line shows the forecasted PV generation. The difference between the forecasted and actual data is due to the lack of cloudiness data.
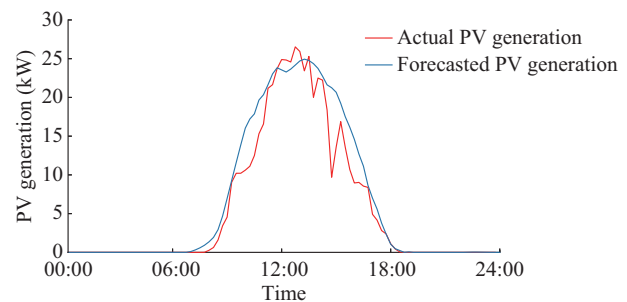

Fig. 2.   Comparison of actual and forecasted PV generations.

The proposed MPC is designed to operate at normal operation state so that the grid is not interrupted. Therefore, the inaccuracy in PV generation and load forecasting causes a suboptimal operation decision. However, this does not constitute any risk of load interruption. More accurate forecasting methods can be utilized in practical applications. In this work, the aim is to utilize MPC for microgrid control considering BSS aging, and hence no special effort is paid to improve the forecasting accuracy. In future works, forecasting method with better accuracy will be employed.

B. BSS Capacity Estimation

The capacity of battery changes with time, which is based on the usage behavior. In literature, there are many heuristic methods utilized to model this behavior [21], [24]. However, those methods are not accurate in real-life practical operations, despite the fact that they reflect dependency of the capacity on environmental conditions and usage behavior. In

this paper, BSS capacity estimator based on least squares method is proposed. The proposed method uses the electrical circuit model of the batteries which is shown in Fig. 3 [35], and estimates model parameters using real-time current and voltage data. The measured quantities provide two linearly independent equations, which do not provide enough redundancy for the solution. Therefore, rather than using a single snapshot of measurements, a time series of measurements are utilized to increase the measurement redundancy. Note that the degradation of the battery lifetime in a day is negligible, and that it may be assumed to be constant within a day. Based on this assumption, the proposed method uses battery terminal voltage and current measurements within a day, and estimates a single usable capacity of BSS.
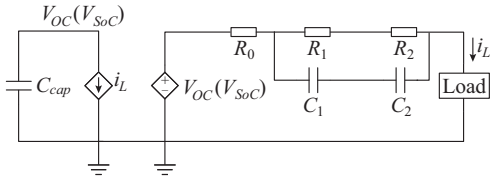

Fig. 3.   Equivalent circuit of battery cell.

In the equivalent circuit of the battery, C_{cap} represents the usable capacity; R_0 represents the instantaneous voltage drop of the step response; R_1, C_1 and R_2, C_2 are responsible for short-time and long-time constants of the step response, respectively; V_{SoC} is the quantitive representation of SoC; V_{OC} varies with V_{SoC} thus the non-linear relationship between V_{OC} and SoC can be modelled. Lastly, a current controlled current source is used to charge/discharge the battery with i_L. The same i_L current flows through C_{cap} and load. Details of the model can be found in [21]. C_{cap} declines as cycle number, discharge current and storage time increases, and is dependent to ambient temperature. Note that the effects of cycle number, discharging current and storage time are reflected automatically in the proposed estimation process, as real measurements are used. In this work, it is assumed that the ambient temperature at the location of the BSS is controlled, and does not change significantly during a day. The left-hand side of Fig. 3 represents the remaining usable capacity of the battery, and a decrease in C_{cap} represents the decrease in lifetime. On the other hand, the right-hand side models *I*-*V* characteristic of the battery. Parallel *RC* circuits yield the transient response. The values of R_0, R_1, R_2, C_1 and C_2 fluctuate with varying SoC values. However, this fluctuating behaviour is negligible for resistive parameters if SoC is 10% or higher [36]. Therefore, in this work, those values are assumed to be constant, and their values can be calculated using the method defined in [24]. The capacitor values are neglected in this study, as steady-state voltage and current measurements are used in the proposed estimator.

The relation between the measurements and system states is given in (1):

$$z = h(x) + e \tag{1}$$

where z is the measurement vector; x is the system state vec-

tor; e is the measurement error vector; and $h(\cdot)$ is the set of functions that relates measurements to the system states.

In this work, z contains battery terminal current and battery terminal energy, which is the product of terminal voltage, supplied current and pre-determined time interval between two measurement updates. As explained previously, to improve measurement redundancy, data recorded during a day with constant time intervals is included in z.

$$z = \begin{bmatrix} i_L[t] \\ i_L[t+1] \\ \vdots \\ i_L[n] \\ E_L[t] \\ E_L[t+1] \\ \vdots \\ E_L[n] \end{bmatrix} \tag{2}$$

where $i_L[t]$ is the terminal current; n is the last time instant when the measurement is taken; $E_L[t] = i_L[t]V_L[t]\Delta t$; $V_L[t]$ is the terminal voltage; and Δt is the time interval between two measurement recordings.

The system states are defined as C_{cap} and SoC voltages corresponding to the measurement update instants values, $V_{SoC}[t]$. The state vector is given below.

$$x = \begin{bmatrix} C_{cap} \\ V_{SoC}[t] \\ V_{SoC}[t+1] \\ \vdots \\ V_{SoC}[n] \end{bmatrix} \tag{3}$$

where $V_{SoC}[t]$ is the SoC voltage at time instant t.

The relation equations between the system states and measurements are defined below. Equations (4) and (5) are obtained based on the Kirchhoff's current law and conservation of the energy law, respectively.

$$i_L[t] = C_{cap}\frac{dV_C}{dt} = C_{cap}\frac{V_{SoC}[t]}{\Delta t} - C_{cap}\frac{V_{SoC}[t-1]}{\Delta t} \tag{4}$$

$$E_L[t] = V_L[t]i_L[t]\Delta t = \frac{1}{2}C_{cap}V_{SoC}^2[t] - i_L^2[t]\left(R_0 + R_1 + R_2\right)\Delta t \tag{5}$$

The least squares estimation problem can be defined as follows:

$$\min r^{\mathrm{T}}r \tag{6}$$

$$\text{s.t. } r = z - h(x) \tag{7}$$

where r is the measurement residual vector. The problem defined in (6) can be solved using the Gauss-Newton iterations, where the states are updated at each iteration as follows:

$$\Delta x_k = G^{-1}H^{\mathrm{T}}\left(z - h(\hat{x}^k)\right) \tag{8}$$

where H is the Jacobian matrix defined in (9); G is the gain matrix and $G = H^{\mathrm{T}}H$; and $\hat{x}^k$ is the estimated system state vector at the kth iteration.

$$H = \begin{bmatrix} \dfrac{\partial i_L[t]}{\partial C_{cap}} & \dfrac{\partial i_L[t]}{\partial V_{SoC}[t]} & \dfrac{\partial i_L[t]}{\partial V_{SoC}[t+1]} & \cdots & \dfrac{\partial i_L[t]}{\partial V_{SoC}[n]} \\[2mm] \dfrac{\partial i_L[t+1]}{\partial C_{cap}} & \dfrac{\partial i_L[t+1]}{\partial V_{SoC}[t]} & \dfrac{\partial i_L[t+1]}{\partial V_{SoC}[t+1]} & \cdots & \dfrac{\partial i_L[t+1]}{\partial V_{SoC}[n]} \\[1mm] \vdots & \vdots & \vdots & & \vdots \\[1mm] \dfrac{\partial i_L[n]}{\partial C_{cap}} & \dfrac{\partial i_L[n]}{\partial V_{SoC}[t]} & \dfrac{\partial i_L[n]}{\partial V_{SoC}[t+1]} & \cdots & \dfrac{\partial i_L[n]}{\partial V_{SoC}[n]} \\[2mm] \dfrac{\partial E_L[t]}{\partial C_{cap}} & \dfrac{\partial E_L[t]}{\partial V_{SoC}[t]} & \dfrac{\partial E_L[t]}{\partial V_{SoC}[t+1]} & \cdots & \dfrac{\partial E_L[t]}{\partial V_{SoC}[n]} \\[2mm] \dfrac{\partial E_L[t+1]}{\partial C_{cap}} & \dfrac{\partial E_L[t+1]}{\partial V_{SoC}[t]} & \dfrac{\partial E_L[t+1]}{\partial V_{SoC}[t+1]} & \cdots & \dfrac{\partial E_L[t+1]}{\partial V_{SoC}[n]} \\[1mm] \vdots & \vdots & \vdots & & \vdots \\[1mm] \dfrac{\partial E_L[n]}{\partial C_{cap}} & \dfrac{\partial E_L[n]}{\partial V_{SoC}[t]} & \dfrac{\partial E_L[n]}{\partial V_{SoC}[t+1]} & \cdots & \dfrac{\partial E_L[n]}{\partial V_{SoC}[n]} \end{bmatrix} \tag{9}$$

Note that temperature change during a day is limited. Therefore, one can consider temperature dependency of the battery capacity by:

1) Dividing the range between the minimum and maximum temperature values of the corresponding day into equal intervals. Note that a few degrees of temperature change is not significantly effective on the battery capacity.

2) Assigning new capacitance states to each of those intervals.

3) Forming (9), also considering those new states.

C. Proposed MGCC Formulation

In MPC, the optimum operation decision for the considered time instant is given based on the forecasted system behavior. In this work, the forecasting horizon is taken as the next 24 hours, and the operation decisions are given in every 15 min, i.e., there are 96 time steps in a forecasting horizon. The proposed method considers the future load demand and PV generation expectations as well as the available BSS capacity, and determines its current operation decision accordingly.

The main concern of the proposed formulation is the overall cost optimization in the system. Therefore, the objective function can be defined in (10).

$$J_t = J_{grid,t} + J_{BSS,aging,t} \tag{10}$$

where $J_{grid,t}$ and $J_{BSS,aging,t}$ are the objective associated with the cost of the power drawn from the grid at time instant t, and the objective associated with the use of BSS at time instant t, respectively. These objective functions can be written in detail as follows:

$$J_{grid,t} = \begin{cases} P_{grid,t}\left(cost_{buy,t}\right)\Delta t & P_{grid,t} \geq 0 \\ P_{grid,t}\left(cost_{sell,t}\right)\Delta t & P_{grid,t} < 0 \end{cases} \tag{11}$$

$$J_{BSS,aging,t} = \frac{Inv_{remain}}{Cycle_{remain}} k \frac{|P_{BSS,t}|\Delta t}{Cap_{usable}} \tag{12}$$

where $P_{grid,t}$ is the power drawn from the grid at time t; $cost_{buy,t}$ is the purchase price of the electricity from the grid; $cost_{sell,t}$ is the selling price of the electricity to the grid;

Inv_{remain} is the price equivalent to the remaining battery life which is defined in (13); k is the penalty factor; $Cycle_{remain}$ is the remaining number of cycles defined in (14); $P_{BSS,t}$ is the power drawn from the BSS at time t; and Cap_{usable} is the BSS capacity estimation, which is found at the end of each day.

$$Inv_{remain} = Inv - A\frac{Inv}{E_{throughput}} \tag{13}$$

$$Cycle_{remain} = Cycle_{max} - Cycle_t \tag{14}$$

where Inv is the capital investment of the BSS; $E_{throughput}$ is the total throughput energy over BSS lifetime; $Cycle_{max}$ is the cycle life of the BSS; $Cycle_t$ is the cycle value that corresponds to the Cap_{usable} in usable capacity vs. cycle number graph at time t; and A is the area under the usable capacity vs. cycle number graph between the installation of BSS and $Cycle_t$ point.

In (11), the energy drawn from the grid is multiplied with the cost of the energy at the corresponding time period. In (12), $|P_{BSS,t}|\Delta t / Cap_{usable}$ presents the effect of depth of discharge (DoD) at the given time instant t, and $Inv_{remain}/Cycle_{remain}$ reflects the updated cost of each cycle. It should be noted that the absolute value of the $P_{BSS,t}$ is used in (12), since it is assumed that the effects of charging and discharging are similar. Finally, penalty factor, k, in (12) is used to represent how much the system operator desires to avoid charging-discharging actions. As the value increases, the proposed MGCC will perform a lower number of actions.

In the given formulation, $Cycle_{remain}$ and Cap_{usable} are calculated by using the developed battery model. The output of the proposed BSS capacity estimation is the Cap_{usable} of the battery. $Cycle_{remain}$ can be found easily by checking the corresponding point in usable capacity versus cycle number graph, provided by the battery manufacturer. A sample graph is given in Fig. 4. It should be noted that in this work, the battery capacity is updated every day by assuming that the aging of BSS in a day is negligibly low.
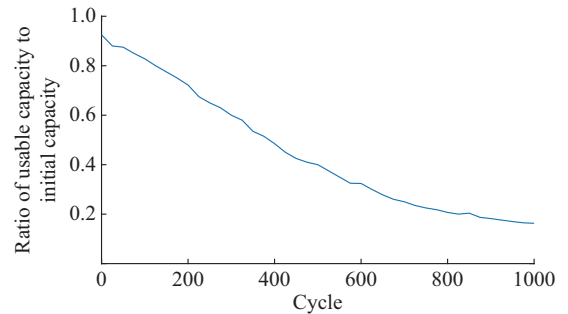

Fig. 4.   Ratio of usable capacity to initial capacity with respect to number of cycles.

The PV panels are also aging throughout their usage. Actually, they are exposing to the environmental conditions more than BSS. However, their performances change due to that the aging can be learned by the LSTM algorithm. Therefore, no extra effort is made in this work on the PV aging.

The constraints of the considered optimization problem

can be given as:

$$P_{load,t} = P_{grid,t} + P_{PV,t} + P_{BSS,t} \tag{15}$$

$$Cap_t = Cap_{t-1} - P_{BSS,t}\Delta t \tag{16}$$

where $P_{load,t}$ is the power demand of the load at time t; $P_{PV,t}$ is the power output of the PV inverters at time t; and Cap_t is the capacity of the BSS at time t.

Equation (15) represents the basic power balance equation for the system, while (16) gives the capacity change in battery depending on the power drawn from battery.

The linearized optimization problem can be written by combining (10)-(16).

$$\min \sum_{t=0}^{96} P_{grid,t}(\cos t_{buy,t})\Delta ts + P_{grid,t}(\cos t_{sell,t})\Delta t(1-s) + \frac{Inv_{remain}}{Cycle_{remain}} \frac{|P_{BSS,t}|\Delta t}{Cap_{usable}} \tag{17}$$

s.t.

$$P_{load,t} = P_{grid,t} + P_{PV,t} + P_{BSS,t} \tag{18}$$

$$0 \le -P_{grid,t} + Ms \tag{19}$$

$$-P_{grid,t} + Ms \le M \tag{20}$$

$$Cap_t = Cap_{t-1} - P_{BSS,t}\Delta t \tag{21}$$

$$P_{BSS,t} \le P_{BSS,\max} \tag{22}$$

$$Cap_t \le Cap_{\max} \tag{23}$$

$$|P_{BSS,t}| \ge 0 \tag{24}$$

$$Cap_t \ge 0 \tag{25}$$

$$s \in \{0, 1\} \tag{26}$$

where s is the binary variable used to check the direction of power flow at grid connection; $|P_{BSS,t}|$ is the absolute value of the variable $P_{BSS,t}$; M is a larger number than the possible power flowing at grid connection; and $P_{BSS,\max}$ is the maximum power capacity of the BSS.

In (21), the initial capacity of the battery should be used at time step $t=0$. While (22) gives the upper and lower bounds of the $P_{BSS,t}$, (23) shows the upper bound of Cap_t. To linearize the conditional cost function (11) a very large number is used, which is namely M. Finally, s is a binary variable, which is used to find either the electricity is bought from the grid or sold to the grid.

In (22), the boundary for $P_{BSS,t}$ is taken as the rated current of BSS, because according to [37], current values larger than the rated current may lead to the fast degradation of BSS, especially in charging mode.

Note that for an optimal operation, all system components should be modeled with the highest accuracy possible. Therefore, it is crucial to estimate the battery capacity, which is the main component in a microgrid that can be utilized for cost optimization, based on the real-time measurements. The proposed capacity estimation method is used to find the optimal model that satisfies the measurements taken. On the other hand, conventional methods use heuristic equations, which may cause significant inaccuracy.

III. SIMULATIONS

In this section, the performance of the proposed BSS capacity estimator will be firstly presented, followed by a comparative study on the application of the proposed MGCC.

In order to observe the performance of the BSS capacity estimator, a test data set is created. Measurement vector is formed adding random error to the measurement set calculated using assumed true states, namely C_{cap} and randomly generated $V_{SoC}[t]$ values.

$V_{SoC}[t]$ values are set to the values given in Table I. The estimated states are given in Table II. At the end of each iteration, the error is calculated. When it is less than the predefined threshold, the estimator is said to be converged. As seen in Table II, the proposed estimator converged in 6 iterations to the unbiased state estimates. Note that as the size of the state vector is 97×1, only three sample V_{SoC} states and corresponding estimates are presented in the table.

TABLE I
TRUE STATES

Variable	Value
C_{cap} (kAh)	100.000
$V_{SoC}[1]$ (V)	12.594
$V_{SoC}[2]$ (V)	12.153
$V_{SoC}[96]$ (V)	15.465

TABLE II
ESTIMATION RESULTS AT EACH ITERATION

No. of iteration	C_{cap} (kAh)	$V_{SoC}[1]$ (V)	$V_{SoC}[2]$ (V)	$V_{SoC}[96]$ (V)
0 (initial value)	80.000	10.000	10.000	10.000
1	114.418	12.594	11.776	18.635
2	109.544	11.786	11.329	15.101
3	101.612	12.371	11.934	15.244
4	99.672	12.623	12.181	15.501
5	100.083	12.585	12.144	15.454
6	100.000	12.597	12.155	15.468

As shown in Tables I and II, the proposed BSS capacity estimator performs with a high accuracy and low computational burden. The method runs daily because BSS capacity does not change significantly within 24 hours. The resulting capacity estimation is supplied to the proposed MGCC to provide the updated limitations on the storage constraints of the optimization problem.

The proposed MGCC is applied to a microgrid that is composed of a load with rated power of 61 kW, and a PV system with a capacity of 55 kWp. During the simulation, the maximum power supplying capability of the BSS is assumed to be 5 kW, and the maximum capacity of BSS is taken as 10 kWh. The initial SoC of BSS is assumed as 20% (2 kWh). The time of use (ToU) tariff is assumed to be 15 cents/kWh from 06:00 to 17:00, 30 cents/kWh from 17:00 to 22:00 and 8 cents/kWh from 22:00 to 06:00. The capital investment of BSS is considered as $5100. Finally, the total throughput power of BSS is taken as 5 MWh.

Five different case scenarios are evaluated using the defined microgrid. All simulations are performed with three-day-long data.

Case 1: The PV system and the BSS are neglected so that all power demand is supplied from the grid. This case actually presents the cost of the required energy to run the load.

Case 2: The PV system is utilized to reduce the electrical cost of the load, but BSS is disregarded.

Case 3: This case includes all components such as the load, PV and BSS. BSS is controlled based on the following rules, which will be stated as the primitive control strategy in the rest of the paper:

1) The battery is charged to 100% between 22:00 and 06:00.

2) The battery starts discharging at 06:00, and re-charging at noon (if the PV generation exceeds the load, the residual amount will be stored for free. If the PV generation is less than the load, the battery will reduce the power demanded from the grid in the morning, and increase the power demanded from the grid in the afternoon. Therefore, the cost will not be affected).

3) At 18:00, the battery starts discharging.

This is the most basic way of controlling a BSS, which is also applied by some commercial products.

Case 4: In this case, BSS is controlled using an MPC-based MGCC. The MGCC does not consider battery aging. This method is similar to the method proposed in [8].

Case 5: This case utilizes the proposed MGCC.

The results are presented in Table III, where the check marks specify whether the corresponding components and features are considered in the control problem for each case.

TABLE III
SIMULATION RESULTS

Case	Grid	PV	BSS	MPC	Aging of BSS	Cost ($)
1	√					563.6
2	√	√				404.1
3	√	√	√			403.9
4	√	√	√	√		395.7
5	√	√	√	√	√	397.1

As shown in Table III, the use of BSS reduces the operation cost of a microgrid. However, Case 3 visualizes that if the battery size is not selected properly in the presence of the primitive control strategy, the cost reduction may be insignificant. Note that if a better battery capacity selection is realized, lower costs would be obtained using primitive control strategy. According to Table III, the forecasting-aided MGCC may provide a significant cost reduction microgrid operation.

The resulting cost for the considered three days is higher if the proposed MGCC is employed as shown from the comparison of Cases 4 and 5. However, if the overall cost which includes battery renewal is considered, it will be seen that the proposed method is superior in terms of cost optimization. Figure 5 shows the load and generation profiles for the considered three days, while Fig. 6 presents the SoC varia-

tions of the battery corresponding to Cases 4 and 5. As shown in Fig. 6, the battery charging cycle number in Case 4 is approximately twice of that of Case 5. Therefore, one can expect to renew the battery sooner if Case 4 is employed.
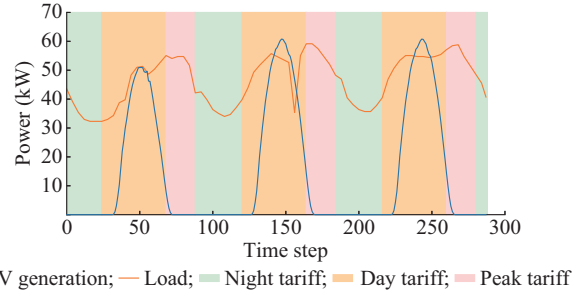

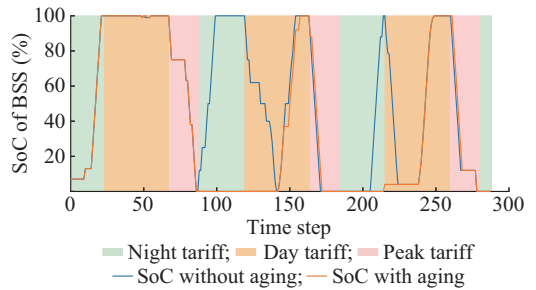Fig. 5.   Actual load and PV generations.

Fig. 6.   Change of SoC with/without aging effect.

Considering the costs obtained in Table III, it can be obtained that BSS will be amortized in five years if Case 4 is employed. This duration will be extended to 6 years with the utilization of Case 5 while the life time of the battery is doubled.

In Table III, errors in load and PV generation forecasting lead to a better operation cost for the proposed method. It can be concluded that the forecasting inaccuracy results in a sub-optimal cost.

The effect of MPC algorithm is shown in Fig. 6. The consideration of the aging effect decreases both the variations in the drawn power from the battery and the depth of discharge. This is an expected observation since the usage of the battery is punished by the added term in cost function given in (12).

IV. CONCLUSION

This paper presents an MGCC based on MPC. The proposed MGCC aims to optimize the operation cost of the microgrid, considering load and PV generation forecasting as well as the up-to-date BSS capacity. In this paper, the optimal control problem is formulated as an MILP problem. The MILP problem minimizes not only the cost of energy but also the battery usage.

Load and PV generation forecasting is realized using Kalman filter and LSTM methods, respectively. As the paper does not concentrate on the improvement of forecasting techniques, no special effort is made to improve the forecasting accuracy.

The optimal usage of BSS is crucially important in microgrid operation. The actual capacity of BSS should be known due to reliability considerations. The conventional heuristic methods provide a rough approximation of the battery capacity, while the proposed capacity estimation method in this work utilizes the well-known electrical battery model and real-time measurements in order to obtain an accurate estimation.

Once the actual usable battery capacity is known, the system operator will utilize BSS to minimize the operation cost to avoid frequent charging and discharging, since those actions significantly reduces the battery life. Considering the high renewal cost of the battery, one must limit those charging and discharging actions to extend the life time of the battery. As seen in the simulations, the proposed MGCC succeeds in reducing the overall cost of the microgrid in longterm operation with the consideration of battery aging.

The major contribution of the paper is the battery model update based on real-time measurements. Note that one can use the proposed battery capacity modeling method in different control strategies without losing generality.

REFERENCES

[1] A. Mills, M. Ahlstrom, M. Brower *et al.*, "Understanding variability and uncertainty of photovoltaics for integration with the electric power system," [Online]. Available: https://escholarship.org/uc/item/58z9s527

[2] D. E. Olivares, A. Mehrizi-Sani, A. H. Etemadi *et al.*, "Trends in microgrid control," *IEEE Transactions on Smart Grid*, vol. 5, no. 4, pp. 1905-1919, Jul. 2014.

[3] A. L. Dimeas and N. D. Hatziargyriou, "Operation of a multiagent system for microgrid control," *IEEE Transactions on Power Systems*, vol. 20, no. 3, pp. 1447-1455, Aug. 2005.

[4] A. Kantamneni, L. E. Brown, G. Parker *et al.*, "Survey of multi-agent systems for microgrid control," *Engineering Applications of Artificial Intelligence*, vol. 45, pp. 192-203, Oct. 2015.

[5] F. Pilo, G. Pisano, and G. G. Soma, "Neural implementation of microgrid central controllers," in *Proceedings of IEEE International Conference on Industrial Informatics (INDIN)*, Vienna, Austria, Jun. 2007, pp. 925-930.

[6] A. Borghetti, M. Bosetti, C. Bossi *et al.*, "An energy resource scheduler implemented in the automatic management system of a microgrid test facility," in *Proceedings of 2007 International Conference on Clean Electrical Power,* Capri, Italy, May 2007, pp. 94-100.

[7] B. Otomega, A. Marinakis, M. Glavic *et al.*, "Model predictive control to alleviate thermal overloads," *IEEE Transactions on Power Systems*, vol. 22, no. 3, pp. 1384-1385, Aug. 2007.

[8] A. Parisio, E. Rikos, and L. Glielmo, "A model predictive control approach to microgrid operation optimization," *IEEE Transactions on Control Systems Technology*, vol. 22, no. 5, pp. 1813-1827, Sept. 2014.

[9] F. Garcia-torres and C. Bordons, "Optimal economical schedule of hydrogen-based microgrids with hybrid storage using model predictive control," *IEEE Transactions on Industrial Electronics*, vol. 62, no. 8, pp. 5195-5207, Aug. 2015.

[10] A. Parisio, E. Rikos, and L. Glielmo, "Stochastic model predictive control for economic/environmental operation management of microgrids: an experimental case study," *Journal of Process Control*, vol. 43, pp. 24-37, Jul. 2016.

[11] B. Zhao, X. Zhang, J. Chen *et al.*, "Operation optimization of standalone microgrids considering lifetime characteristics of battery energy storage system," *IEEE Transactions on Sustainable Energy*, vol. 4, no. 4, pp. 934-943, Oct. 2013.

[12] M. Pereira, D. M. De La Pena, and D. Limon, "Robust economic model predictive control of a community micro-grid," in *Proceedings of 2016 IEEE 55th Conference on Decision and Control,* Las Vegas, USA, Dec. 2016, pp. 2739-2744.

[13] T. Morstyn, B. Hredzak, R. P. Aguilera *et al.*, "Model predictive control for distributed microgrid battery energy storage systems," *IEEE Transactions on Control Systems Technology*, vol. 26, no. 3, pp. 1107-1114, May 2018.

[14] Y. Zheng, S. Li, and R. Tan, "Distributed model predictive control for on-connected microgrid power management," *IEEE Transactions on Control Systems Technology*, vol. 26, no. 3, pp. 1028-1039, May 2018.

[15] W. Shi, N. Li, C. C. Chu *et al.*, "Real-time energy management in microgrids," *IEEE Transactions on Smart Grid*, vol. 8, no. 1, pp. 228-238, Jan. 2017.

[16] S. Jena, P. Sinha, P. R. Satpathy *et al.*, "Performance analysis of solar PV based microgrid with and without BESS estimating the expected battery life," in *Proceedings of International Conference on Technologies for Smart City Energy Security and Power: Smart Solutions for Smart Cities*, Bhubaneswar, India, Mar. 2018, pp. 1-6.

[17] D. W. Dees, V. S. Battaglia, and A. Bélanger, "Electrochemical modeling of lithium polymer batteries," *Journal of Power Sources*, vol. 110, no. 2, pp. 310-320, Aug. 2002.

[18] J. Newman, K. E. Thomas, H. Hafezi *et al.*, "Modeling of Lithium-ion batteries," *Journal of Power Sources*, vol. 119-121, pp. 838-843, Jun. 2003.

[19] P. Rong, S. Member, and M. Pedram, "An analytical model for predicting the remaining battery capacity of Lithium-ion batteries," *IEEE Transactions on Very Large Scale Integration (VLSI) Systems*, vol. 14, no. 5, pp. 1-12, May 2006.

[20] R. Rynkiewicz, "Discharge and charge modeling of lead acid batteries," in *Proceedings of 14th Annual Applied Power Electronics Conference and Exposition (Cat. No.99CH36285)*, Dallas, USA, Aug. 1999, pp. 707-710.

[21] G. A. Rincón-mora, "An accurate electrical battery model capable of predicting lifetime and *I-V* performance motivation," *IEEE Transactions on Energy Conversion*, vol. 21, no. 2, pp. 1-8, Jun. 2005.

[22] C. Guenther, J. K. Barillas, S. Stumpp *et al.*, "A dynamic battery model for simulation of battery-to-grid applications," in *Proceedings of IEEE PES Innovative Smart Grid Technologies Conference Europe*, Berlin, Germany, Oct. 2012, pp. 1-7.

[23] L. W. Yao, P. Y. Kong, and N. R. N. Idris, "Modeling of Lithium-ion battery using MATLAB/Simulink," in *Proceedings of 39th Annual Conference of the IEEE Industrial Electronics Society*, Vienna, Austria, Jan. 2013, pp. 1729-1734.

[24] H. Zhang and M. Y. Chow, "Comprehensive dynamic battery modeling for PHEV applications," in *Proceedings of IEEE PES General Meeting,* Providence, USA , Jul. 2010, pp. 1-6.

[25] S. Boulmrharj, Y. NaitMalek, A. E. Mouatamid *et al.*, "Towards a battery characterization methodology for performance evaluation of microgrid systems," in *Proceedings of 2018 International Conference on Smart Energy Systems and Technologies,* Sevilla, Spain, Oct. 2018, pp. 1-6.

[26] M. U. Gudelek, C. R. Cirak, E. Arin *et al.*, "Load and PV generation forecast based cost optimization for nanogrids with PV and battery," in *Proceedings of 53rd International Universities Power Engineering Conference*, Glasgow, United Kingdom, Dec. 2018, pp. 1-6.

[27] J. B. Rawlings and D. Q. Mayne, *Model Predictive Control: Theory and Design*, vol. 1. Cheryl M. Rawlings, 2009.

[28] D. Park, M. El-Sharkawi, R. Marks *et al.*, "Electric load forecasting using an artificial neural network," *IEEE Transactions on Power Systems*, vol. 6, no. 2, pp. 442-449, May 1991.

[29] A. Ahmad, N. Javaid, M. Guizani *et al.*, "An accurate and fast converging short-term load forecasting model for industrial applications in a smart grid," *IEEE Transactions on Industrial Informatics*, vol. 13, pp. 2587-2596, Oct. 2017.

[30] C. M. Lee and C. N. Ko, "Short-term load forecasting using lifting scheme and ARIMA models," *Expert Systems with Applications*, vol. 38, no. 5, pp. 5902-5911, May 2011.

[31] H. Nie, G. Liu, X. Liu *et al.*, "Hybrid of ARIMA and SVMs for short-term load forecasting," *Energy Procedia*, vol. 16, PART C, pp. 1455-1460, Apr. 2012.

[32] Y. Z. Li, R. Q. Nie, and J. C. Niu, "Forecast of power generation for grid-connected photovoltaic system based on knowledge representation of rough sets," in *Proceedings of Asia-Pacific Power and Energy Engineering Conference,* Shanghai, China, Sept. 2012, pp. 9-12.

[33] N. Sharma, P. Sharma, D. Irwin *et al.*, "Predicting solar generation from weather forecasts using machine learning," in *Proceedings of IEEE International Conference on Smart Grid Communications*, Brussels, Belgium, Oct. 2011, pp. 528-533.

[34] A. Fentis, L. Bahatti, M. Mestari *et al.*, "Short-term PV power forecasting using support vector regression and local monitoring data," in *Proceedings of International Renewable and Sustainable Energy Conference*, Marrakech, Morocco, Jul. 2016, pp. 1092-1097.

[35] A. Rahmoun and H. Biechl, "Modelling of Li-ion batteries using equivalent circuit diagrams," *Electrical Review*, vol. 88, pp. 152-156,

Jan. 2013.

[36] J. D. Dogger, B. Roossien, and F. D. J. Nieuwenhout, "Characterisation of Li-ion batteries for intelligent management of distributed grid-connected storage," *IEEE Transactions on Energy Conversion*, vol. 26, no. 1, pp. 256-263, Mar. 2011.

[37] S. S. Choi and H. S. Lim, "Factors that affect cycle-life and possible degradation mechanisms of a Li-ion cell based on LiCoO$_2$," *Journal of Power Sources*, vol. 111, no. 1, pp. 130-136, Sept. 2002.

Ugur Can Yilmaz received his B.Sc. degree in electrical and electronics engineering from Middle East Technical University (METU), Ankara, Turkey, in 2018. He is currently an M.Sc. student in METU, Ankara, Turkey. His main areas of research are power system modeling and state estimation in distribution systems.

Mustafa Erdem Sezgin received the B.Sc. and M.Sc. degrees in electrical and electronics engineering from METU, Ankara, Turkey, in 2015 and 2017, respectively. Currently he is a Ph.D. student and research assistant at METU, Ankara, Turkey. His main areas of research include power system modeling and microgrid control.

Murat Gol received the B.Sc.(2007) and M.Sc.(2009) degrees in electrical and electronics engineering from METU, Ankara, Turkey. He received his Ph.D. degree from Northeastern University, Boston, USA in 2014. Currently he is an associate professor and a member of Center for Solar Energy Research and Applications in METU. His main research areas are power system modeling, power system state estimation, and real-time monitoring and control of power systems.